

Zadoff-Chu Coded Ultrasonic Signal for Accurate Range Estimation

Mohammed H. AlSharif¹, Mohamed Saad¹, Mohamed Siala², Tarig Ballal¹, Hatem Boujemaa², Tareq Y. Al-Naffouri¹

¹King Abdullah University of Science & Technology (KAUST), Thuwal, Saudi Arabia

²Higher School of Communication of Tunis (SUP'COM), University of Carthage, Tunisia

{mohammed.alsharif, mohamed.saadeldin, tarig.ahmed, tareq.alnaffouri}@kaust.edu.sa

{mohamed.siala, boujemaa.hatem}@supcom.tn

Abstract—This paper presents a new adaptation of Zadoff-Chu sequences for the purpose of range estimation and movement tracking. The proposed method uses Zadoff-Chu sequences utilizing a wideband ultrasonic signal to estimate the range between two devices with very high accuracy and high update rate. This range estimation method is based on time of flight (TOF) estimation using cyclic cross correlation. The system was experimentally evaluated under different noise levels and multi-user interference scenarios. For a single user, the results show less than 7 mm error for 90% of range estimates in a typical indoor environment. Under the interference from three other users, the 90% error was less than 25 mm. The system provides high estimation update rate allowing accurate tracking of objects moving with high speed.

I. INTRODUCTION

Estimating the range between two devices with high accuracy is a very important tool in many modern technologies. It has applications in consumer electronics, medical care, advertisement, gesture controlled devices, navigation tools, location aware sensor networks and many other applications. Range estimation can be implemented using methods that are based on ultrasonic, radio signal, infrared, or lasers [1], [2], [3], [4]. Infrared and laser ranging systems have high accuracy but they are complex and expensive. Radio signal based ranging algorithms mainly use received signal strength or time of arrival. Received signal strength methods utilizing Wi-Fi or Bluetooth require pre-calibration and provide poor ranging accuracy [5]. Time of arrival based methods require accurate synchronization since small timing errors result in very high ranging errors. Recent ultra-wideband ranging systems reported 10-20 cm ranging accuracy [6], but their accuracy degrades significantly in non-line of sight scenarios. Ultrasonic ranging is of low cost and has high accuracy due to the low speed of ultrasonic signal which enables us to estimate range with high accuracy based on time of flight (TOF). The speed of sound can change with humidity and temperature but these changes are negligible in a typical indoor environment [7]. The coverage of ultrasonic ranging is limited to the energy of the transmitted signal and having line of sight between the transmitter and the receiver [8].

This work is supported by the KAUST-MIT-TUD consortium under grant OSR-2015-Sensors-2700.

In [9], Figueroa F. and Barbieri E. used a narrowband ultrasonic signal to measure the distance between two transducers using the phase difference between the transmitted and the received signals. Huang in [10] presented an algorithm for high resolution phase-shift-based range estimation using a narrowband multiple frequency continuous wave (MFCW) ultrasonic signal. In [11], Hua H. proposed a low-cost dynamic range estimation device based on phase shift detection using a narrowband amplitude modulated ultrasonic signal. The main drawback of using phase-shift method is that the maximum estimated range is limited to one wavelength of the transmitted signal. Narrowband ultrasonic ranging accuracy decreases significantly in noisy environments and is sensitive to multipath and interference.

There is a number of TOF based ranging systems reported in the literature that utilize wideband ultrasonic signals to mitigate for narrowband signal limitations. In [7] Girod L. developed an ultrasonic ranging system that performs well in the presence of many types of interference using a wideband chirp signal. In [12], Hazas M. developed a TOF based range estimation system utilizing wideband spectrum with direct sequence spread spectrum (DSSS) modulation to improve ranging accuracy in noisy environments. In [13] Saad M. presented a high accuracy TOF based range estimation algorithm using frequency hopping spread spectrum (FHSS). The system can achieve sub-sample ranging resolution utilizing phase correction algorithm. In [14] F. Alvarez, developed a CDMA-based acoustic local positioning system using TOF estimation.

Generally TOF can be estimated by locating the peak of the cross correlation between the transmitted signal and the received signal, provided that the transmitter and the receiver are synchronized. This synchronization can be achieved using radio frequency signals or by sharing the same clock between the ultrasonic transmitter and the receiver. The distance between the transmitter and the receiver can then be found by multiplying the TOF by the speed of sound.

This paper proposes a TOF-based range estimation system of high accuracy by utilizing Zadoff-Chu sequences. These sequences are widely used in Long Term Evolution (LTE) air interface in the Primary Synchronization Signal (PSS). The proposed system adapts the usage of Zadoff-Chu sequences

with ultrasonic signals to the purpose of range estimation of static and moving objects. Compared to the previous work on range estimation, the proposed method contributes to the following:

- Use of Zadoff-Chu sequences to generate wideband ultrasonic signals for range estimation with high accuracy.
- Utilizing Zadoff-Chu sequence properties to combat noise and allow for multi-user system.
- Increasing the system update rate by utilizing the periodicity of Zadoff-Chu sequences and using cyclic shift cross correlation.
- Experimental evaluation of the range estimation system in an indoor environment using low cost hardware.

In the second section of the paper, overview of the proposed system and the signal design are presented. The third section explains the signal processing techniques that are used to estimate the range. The experimental set up used in this work is presented in the fourth section. The fifth section shows the range estimation results for static and moving targets under different noise and interference scenarios. The last section concludes the paper.

II. SIGNAL DESIGN

A. Overview

The proposed system estimates the range of static and moving objects using a wideband ultrasonic signal with a central frequency at 20 kHz and a bandwidth of 7 kHz which are dictated by the hardware used in this work. There are several factors that can affect range estimation accuracy such as signal to noise ratio (SNR), interference from other systems and multi-path reflections. Signal design should provide immunity to noise and multi-path, allow for multi-user system. For these reasons, the proposed system utilizes Zadoff-Chu sequences that have good cross correlation properties and provide each user with a unique sequence.

B. Zadoff-Chu

Zadoff-Chu sequence is a polyphase complex valued sequence, named after Solomon A. Zadoff and D.C. Chu [15],[16]. Zadoff-Chu sequences are constant amplitude zero auto-correlation (CAZAC) sequences, where the auto-correlation is zero for any nonzero lag. A Zadoff-Chu sequence s_k of length N can be written in the following form [16]:

$$s_k = e^{i\alpha_k}, \quad k = 0, 1, 2, \dots, N-1, \quad (1)$$

where α_k is given by:

$$\alpha_k = \begin{cases} \frac{M\pi k^2}{N}, & \text{if } N \text{ is even} \\ \frac{M\pi k(k+1)}{N}, & \text{if } N \text{ is odd} \end{cases} \quad (2)$$

where M and N are integers and M is coprime to N .

The received signal is modeled as:

$$y[k] = \alpha x[k-d] + w[k], \quad (3)$$

where α is an attenuation factor, $x[k]$ is the transmitted signal, d is the delay between transmitting and receiving the signal

and $w[k]$ is an additive white Gaussian noise (AWGN). If the transmitted signal is an odd-length Zadoff-Chu sequence, $y[k]$ can be written as:

$$y[k] = \alpha e^{i\pi \frac{M}{N}(k-d)(k-1-d)} + w[k], \quad k = 1, 2, \dots, N \quad (4)$$

The cross-correlation of x with y is given by:

$$(x * y)[n] \triangleq \sum_{m=0}^{N-1} x^*[m]y[m+n] \quad (5)$$

The cross correlation function $r[n]$ is given by:

$$\begin{aligned} r[n] &= \sum_{k=0}^{N-1} x^*[k]y[k+n] \\ &= \sum_{k=0}^{N-1} e^{-i\pi \frac{M}{N}k(k+1)} \left(\alpha e^{i\pi \frac{M}{N}(k+n-d)(k+1+n-d)} \right. \\ &\quad \left. + w[k+n] \right) \end{aligned}$$

Considering the noiseless case and with some manipulations we can reduce the summation to:

$$r[n] = \alpha e^{i\pi \frac{M}{N}(n-d)(n+1-d)} \sum_{k=0}^{N-1} e^{-i\pi \frac{M}{N}2k(n-d)} \quad (6)$$

Taking the absolute value of the cross-correlation function, we have:

$$\begin{aligned} |r[n]| &= |\alpha| \left| \sum_{k=0}^{N-1} e^{-i\pi \frac{M}{N}2k(n-d)} \right| \\ &= |\alpha| \left| \frac{e^{-i2\pi M(n-d)} - 1}{e^{-i2\pi \frac{M}{N}(n-d)} - 1} \right| \\ &= \begin{cases} 0 & \text{if } n \neq d \\ |\alpha|N & \text{if } n = d \end{cases} \end{aligned}$$

note that M and N are coprime. The peak of the cross correlation is at the TOF ($n = d$). The same derivations can be implemented to even-length Zadoff-Chu sequences.

Since the signal bandwidth $BW = \frac{2}{T_{sym}}$, where T_{sym} is symbol duration, the minimum symbol duration depends on the available bandwidth. The hardware used in this work has a total bandwidth of 7 kHz, limiting the symbol duration not to be less than 0.286 ms. The sequence in this work has been chosen to have a length of 15 symbols ($N = 15$) and a symbol duration of 0.3125 ms, resulting a sequence duration of 4.688 ms. For continuous transmission, this sequence is repeated P times, where each single sequence is referred to as a block.

III. SIGNAL PROCESSING

This section presents the modulation and demodulation of Zadoff-Chu sequences. Then the direct path estimation using cross correlation and earliest peak search is explained. Finally the use of periodicity of Zadoff-Chu sequences and cyclic shift cross correlation are shown for controlling the system update rate and combating noise by averaging.

A. Complex Signal Modulation and Demodulation

A single block consisting of Zadoff-Chu sequence of 15 symbols is generated ($N = 15$ and $M = 1$) based on Equation (2). This sequence is upsampled to the system sampling rate 192 kHz. The real part is modulated using a cosine wave with carrier frequency of 20 kHz and the imaginary part is modulated using a sine wave with the same carrier frequency. The resulted signal is fed to the transmitter.

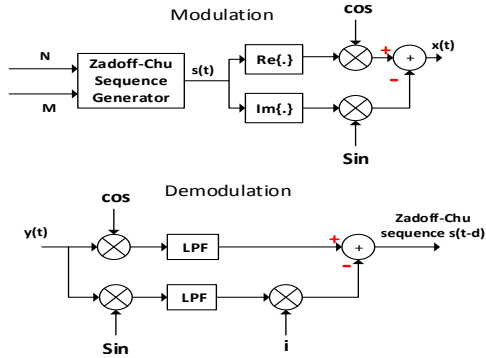


Fig. 1. Modulation and Demodulation schemes

The received signal is demodulated to retrieve the delayed Zadoff-Chu sequence. Modulation and demodulation steps are illustrated in figure 1.

B. Direct Path Estimation

Assuming multi-paths reception, the received signal in (3) can be written as

$$y[k] = \sum_{i=1}^L \alpha_i x[k - d_i] + w[k]. \quad (7)$$

A cross-correlation between a reference block and a window of the received signal is applied to estimate the TOF of the first block. The peak associated with the direct path is not necessarily the highest peak, multi-paths can add up constructively and result in a higher peak. However, the direct path peak is always the first significant peak to arrive. Cross correlating the reference transmitted block with the received blocks results in peaks at d_1, d_2, \dots, d_L , with $d_1 < d_i$, $i = 2, 3, \dots, L$. In order to find the peak corresponding to the TOF of the first block, an early peak search is applied where the highest peak is located, then a search for all the earliest peak with amplitude greater than a threshold of 0.6 of the highest peak is performed. This threshold was tested experimentally and proved to be high enough to avoid noise, and low enough for direct path detection. Once the TOF, d_1 , of the direct path has been estimated, the distance to the target is given by

$$D = d_1 \frac{v_s}{f_s}, \quad (8)$$

where v_s is the speed of sound in air. Figure 2 illustrates this step.

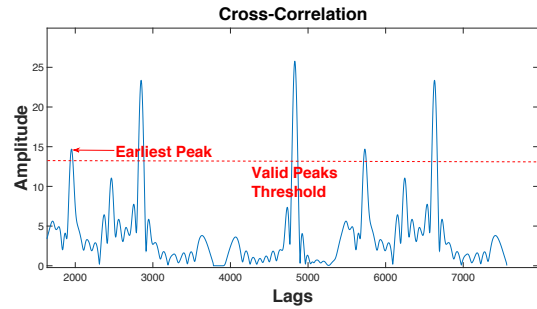


Fig. 2. Multiple cross-correlation peaks with earliest peak search

At the start the cross correlation window is set to allow for the maximum targeted range. The window is then shrunk to a narrower width around the previous estimate. This width should be larger than the maximum distance traveled by the target in one block duration. This reduces the computational complexity of the system and the amount of multi-paths included.

C. Cyclic Shift Cross Correlation

Utilizing continuous signal transmission and the periodicity of Zadoff-Chu sequences, cyclic shift cross correlation can be applied to increase the system update rate. In cyclic shift cross correlation, cyclic shifted versions of the transmitted block are generated and correlated with the corresponding windows of the received signal as illustrated in figure 3. With the use of

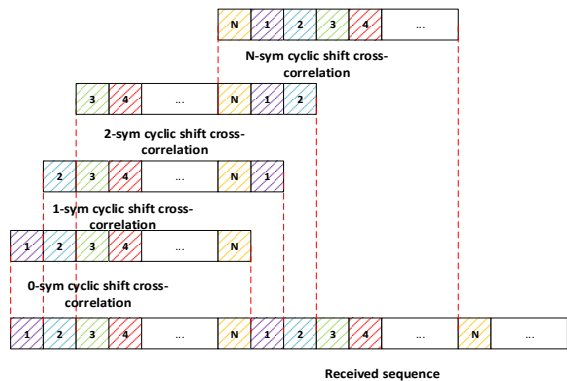


Fig. 3. Cyclic shift cross correlation illustration

cyclic cross correlation, system update rate can be increased from $\frac{1}{T_{block}}$ up to $\frac{N}{T_{block}}$ where T_{block} refers to the duration of the block ($T_{block} = 4.688$ ms). Providing high update rate is useful in two folds; allowing tracking of fast moving objects and improving ranging accuracy by averaging.

IV. EXPERIMENTAL SETUP

This section presents the experimental setup used for testing and evaluating the system. The transmitters (Tx) used are

Clarion SRG213H tweeters, which have a bandwidth of 7 kHz centered at 20 kHz. Microphones on a customized board, are used as receivers (Rx). Both Tx and Rx are connected to a PC through a sound-card. The sound-card used is E44 Express card providing sampling rate up to 192 kHz. During experiments, data is recorded as .wav files and saved in the PC to be processed off-line using MATLAB. The experimental setup is installed in a typical indoor environment with dimensions 300 cm × 300 cm × 400 cm. The changes in humidity and temperature are negligible over the duration of the experiments. Thus sound velocity is assumed to be constant during the experiments (345.66 m/s).

To provide a benchmark for evaluating the performance of the proposed system, an infrared-based tracking system is used to give ground truth for the range between Tx and Rx with 0.1 mm resolution. The used infrared-based system is ARTTRACK which gives 6 degrees of freedom and has a maximum update rate of 300 Hz [17]. This system uses a set of IR cameras (up to 8 cameras) to keep track of retro-reflective film coated small spheres providing accurate 3D location and orientation. Figure 4 shows the experimental setup.

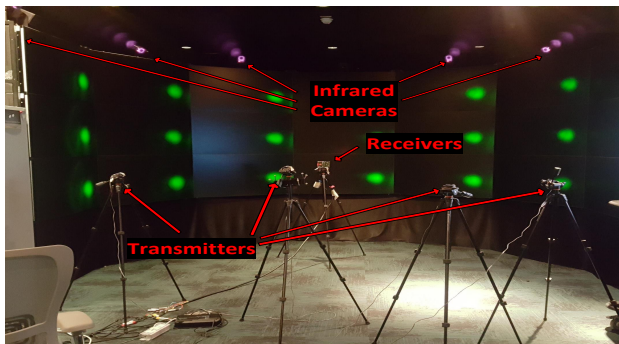


Fig. 4. Experimental setup

V. RESULTS

In this section, the proposed system performance is evaluated by presenting experimental results under different scenarios. A single Rx was fixed in a certain location and a Tx was moved between six different locations. For each location, a signal of 100 blocks was transmitted and this was repeated 10 times, giving a total of 1000 transmitted blocks. The SNR was varied from 20 dB to -20 dB by adding AWGN to the received signal. Figure 5 shows the percentage of estimates with error less than x mm for different SNRs. Tables I and II show the root mean square error (RMSE) and variance (σ^2) for the estimated range at the six different locations for different SNRs. The results show high ranging accuracy in most cases with 75% error less than 5 mm and 9.5 mm for 20 dB and -20 dB respectively. As SNR decreases the accuracy slightly degrades, but the system still provides high accuracy with low SNR.

The performance of the system was tested in the presence of interference from other systems that are using different Zadoff-Chu sequences. Figure 6 shows the percentage of estimates

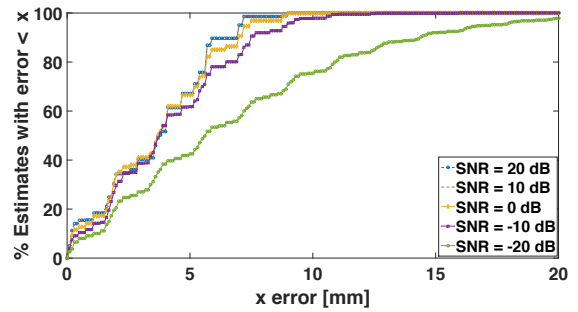


Fig. 5. Percentage of estimates with error less than X for different SNRs

Distance (mm)	RMSE mm				
	SNR 20 dB	10 dB	0 dB	-10 dB	-20 dB
575.9	5.13	5.16	5.36	5.98	8.02
986.1	4.23	4.21	4.10	4.66	7.56
2149.6	1.49	1.53	1.84	2.78	8.30
2501.3	3.43	3.44	3.62	4.34	8.77
2860.8	5.33	5.34	5.67	6.05	9.40
3510.4	5.69	5.63	5.73	5.83	9.58

TABLE I

RANGE RMSE CALCULATED AT DIFFERENT SNR VALUES

Distance (mm)	Variance (mm)				
	SNR 20 dB	10 dB	0 dB	-10 dB	-20 dB
575.9	2.88	2.99	4.14	7.68	45.47
986.1	1.95	2.08	2.41	6.36	45.22
2149.6	2.16	2.22	3.29	7.62	68.67
2501.3	4.66	4.50	5.98	8.94	66.59
2860.8	6.82	6.96	8.90	14.61	74.14
3510.4	2.95	2.93	3.99	9.26	60.65

TABLE II

RANGE VARIANCE CALCULATED AT DIFFERENT SNR VALUES

with error less than X mm for different multi-user interference scenarios. Table III shows the RMSE and variance in range estimation in three interference scenarios; one-user, two-users and three-users. The three interfering users were located at 2.28 m, 1.98 m and 2.11 m away from the receiver respectively. At each scenario, 1000 blocks were transmitted and processed to obtain range estimates. Ranging accuracy slightly decreases with increasing number of interfering users, though the results show high robustness to multi-user interference with 75% error less than 5 mm and 15 mm for single user and four users respectively.

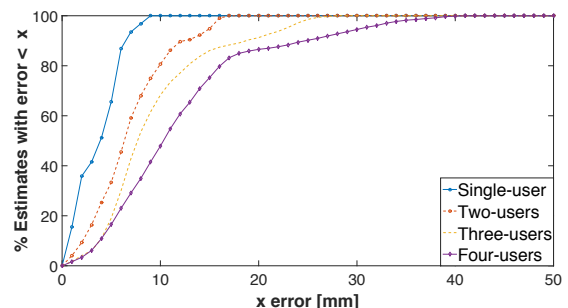


Fig. 6. Percentage of estimates with error less than X in multi-user scenario

Distance (mm)	1-user interference		2-users interference		3-users interference	
	RMSE (mm)	σ^2 (mm)	RMSE (mm)	σ^2 (mm)	RMSE (mm)	σ^2 (mm)
575.9	5.42	2.56	5.34	3.17	5.47	3.39
986.1	7.34	1.53	8.32	3.63	9.94	6.20
2149.6	4.37	3.07	7.77	5.71	11.18	8.63
2501.3	4.54	6.73	8.33	7.00	13.12	7.23
2860.8	13.64	5.90	20.96	15.04	28.83	30.94
3510.4	9.72	2.43	11.67	8.61	13.67	11.19

TABLE III
RANGE RMSE AND VARIANCE CALCULATED AT MULTI-USER SCENARIO

Movement	max speed (mm/sec)	RMSE (mm)	% error < 10 mm	% error < 30 mm	% error < 50 mm
Slow	1139	14.79	38	97	100
Fast	1837.4	23.00	40	78.12	97.08
Very fast	2067.6	24.66	8	79	93

TABLE IV
EVALUATION OF DYNAMIC RANGE ESTIMATION

The performance of the system was evaluated in tracking moving object at different speeds. Rx was fixed in one location, and Tx was moved with different speeds. Table IV summarizes RMSE and percentage range estimates with error less than 10 mm, 30 mm, and 50 mm at three different speeds. The results show that the proposed algorithm provides high tracking accuracy for objects moving with different speeds. Figures 7, 8, 9, and 10 show the estimated range using three receivers and the ground truth. The ground truth plot is obscured by the other plots. We can see that the estimated range is very accurate for the three speeds.

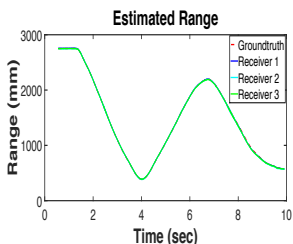


Fig. 7. Estimated range of object moving with slow speed

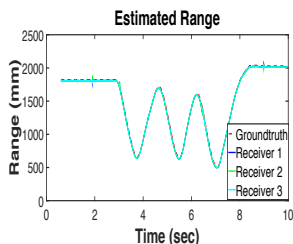


Fig. 8. Estimated range of object moving with very fast speed

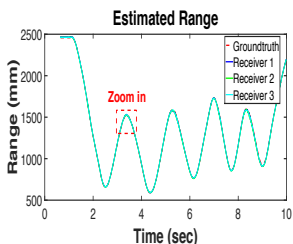


Fig. 9. Estimated range of object moving with fast speed

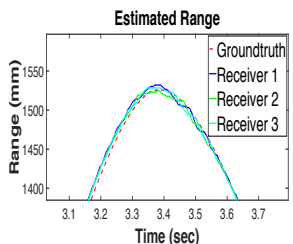


Fig. 10. Zoom-in estimated range of object moving with fast speed

VI. CONCLUSION

A new adaptation of Zadoff-Chu sequences in high accuracy range estimation and movement tracking utilizing wideband ultrasonic signals has been implemented. This algorithm uses cross correlation with earliest peak detection in an efficient

way to reduce complexity while providing high ranging accuracy. The system utilizes the periodicity of Zadoff-Chu sequences and cyclic cross correlation to provide higher update rate and improve immunity to noise by averaging. The performance of the system was evaluated experimentally using low cost hardware in a typical indoor environment. The results show that the system is robust and accurate even in the low SNR scenario or strong multi-user interference. The system has high ranging accuracy in most cases with 75% error less than 9.5 mm for -20 dB and with 75% error less than 5 mm and 15 mm for single user and four users respectively. Also the system has high accuracy for tracking objects moving with high speed.

REFERENCES

- [1] J. Hightower and G. Borriello, "A survey and taxonomy of location systems for ubiquitous computing," *IEEE computer*, vol. 34, no. 8, pp. 57–66, 2001.
- [2] K. Whitehouse, C. Karlof, and D. Culler, "A practical evaluation of radio signal strength for ranging-based localization," *ACM SIGMOBILE Mobile Computing and Communications Review*, vol. 11, no. 1, pp. 41–52, 2007.
- [3] Ç. Yüzbaşıoğlu and B. Barshan, "Improved range estimation using simple infrared sensors without prior knowledge of surface characteristics," *Measurement Science and Technology*, vol. 16, no. 7, p. 1395, 2005.
- [4] M.-C. Amann, T. Bosch, M. Lescure, R. Myllyla, and M. Rioux, "Laser ranging: a critical review of usual techniques for distance measurement," *Optical engineering*, vol. 40, no. 1, pp. 10–19, 2001.
- [5] M. Cypriani, F. Lassabe, P. Canalda, and F. Spies, "Open wireless positioning system: A wi-fi-based indoor positioning system," in *Vehicular Technology Conference Fall (VTC 2009-Fall)*, *IEEE 70th*, 2009, pp. 1–5.
- [6] R. M. Narayanan and M. Dawood, "Doppler estimation using a coherent ultrawide-band random noise radar," *IEEE Transactions on Antennas and Propagation*, vol. 48, no. 6, pp. 868–878, 2000.
- [7] L. Girod and D. Estrin, "Robust range estimation using acoustic and multimodal sensing," in *Proceedings of Intelligent Robots and Systems, 2001. 2001 IEEE/RSJ International Conference on*, vol. 3. IEEE, 2001, pp. 1312–1320.
- [8] M. Kushwaha, K. Molnár, J. Sallai, P. Volgyesi, M. Maróti, and A. Lédeczi, "Sensor node localization using mobile acoustic beacons," in *IEEE International Conference on Mobile Adhoc and Sensor Systems Conference*, 2005, pp. 9–17.
- [9] F. Figueroa and E. Barbieri, "An ultrasonic ranging system for structural vibration measurements," *IEEE Transactions on Instrumentation and Measurement*, vol. 40, no. 4, pp. 764–769, 1991.
- [10] C. Huang, M. Young, and Y. Li, "Multiple-frequency continuous wave ultrasonic system for accurate distance measurement," *Review of scientific instruments*, vol. 70, no. 2, pp. 1452–1458, 1999.
- [11] H. Hua, Y. Wang, and D. Yan, "A low-cost dynamic range-finding device based on amplitude-modulated continuous ultrasonic wave," *IEEE Transactions on Instrumentation and Measurement*, vol. 51, no. 2, pp. 362–367, 2002.
- [12] M. Hazas and A. Ward, "A novel broadband ultrasonic location system," pp. 264–280, 2002.
- [13] M. M. Saad, C. J. Bleakley, and S. Dobson, "Robust high-accuracy ultrasonic range measurement system," *IEEE Transactions on Instrumentation and Measurement*, vol. 60, no. 10, pp. 3334–3341, 2011.
- [14] F. J. Álvarez, T. Aguilera, and R. López-Valcarce, "Cdma-based acoustic local positioning system for portable devices with multipath cancellation," *Digital Signal Processing*, vol. 62, pp. 38–51, 2017.
- [15] R. Frank, S. Zadoff, and R. Heimiller, "Phase shift pulse codes with good periodic correlation properties (corresp.)," *IRE Transactions on Information Theory*, vol. 8, no. 6, pp. 381–382, 1962.
- [16] D. Chu, "Polyphase codes with good periodic correlation properties (corresp.)," *IEEE Transactions on Information Theory*, vol. 18, no. 4, pp. 531–532, 1972.
- [17] <http://www.ar-tracking.com/products/tracking-systems/systems-overview/>. (2017) Artrack system overview. [Online]. Available: <http://www.ar-tracking.com/products/tracking-systems/systems-overview/>